

****TITLE****
*ASP Conference Series, Vol. **VOLUME**, **PUBLICATION YEAR***
****EDITORS****

HST/STIS Spectroscopy of 3C 273

S. R. Heap, G. M. Williger

Code 681, NASA's Goddard Space Flight Center, Greenbelt MD 20771

R. Davé

Steward Observatory, University of Arizona

R. J. Weymann

Carnegie Observatories (OCIW)

E. B. Jenkins, T. M. Tripp

Princeton University Observatory

Abstract. We present preliminary results on the low-redshift Ly α forest as based on STIS spectra of 3C 273. A total of 121 intergalactic Ly α -absorbing systems were detected, of which 60 are above the 3.5σ completeness limit, $\log N_{\text{HI}} \approx 12.3$. The median line-width parameter, $b = 27$ km/s, is similar to that seen at high redshift. However the distribution of HI column densities has a steeper slope, $\beta = 2.02 \pm 0.21$, than is seen at high redshift. Overall, the observed $N_{\text{HI}}-b$ distribution is consistent with that derived from a Λ CDM hydrodynamic simulation.

1. Introduction

3C273 is the most closely observed target for studies of the Ly α forest at low-redshift. As shown in Table 1 (next page), it has been observed by FUSE and each of the Hubble spectrographs – FOS, GHRS, and in this past year, the Space Telescope Imaging Spectrograph (STIS). It is a cinch for early observation with the Cosmic Origins Spectrograph (COS) scheduled to be installed on HST in early 2004. This interest in 3C273 is for good reason: as the brightest AGN at a significant redshift ($z=0.158$) in the sky, it offers the best opportunity to explore the low-redshift Ly α forest. This opportunity was not lost on Ray and John Bahcall. In fact, the first major result of HST came from GHRS and FOS spectroscopy of 3C 273: the rate of evolution of absorbers, i.e. the rate at which absorbers of a given column density disappear from view, slows dramatically at $z < 2$ (Morris et al. 1991; Bahcall et al. 1991). The survival of HI-absorbing systems to the present epoch, which was predicted by Ray and his colleagues (Bechtold, Weymann et al. 1987), is thought to be a consequence of a lower ionizing background at $z < 2$, reflecting a decline in the quasar population after $z \sim 2$ (Davé et al. 1999).

Cosmological simulations indicate that low- z and high- z absorbing systems having the same column density belong to different density/structure regimes. For example, an absorption feature of a given column density arising in a filament in the low- z IGM would arise in a relative void at high-redshift. This puts investigators of the low- z IGM at a disadvantage with respect to our high- z colleagues. We have to pry out weak absorption features to explore physical systems that would produce saturated absorbers at high redshift. This is why the STIS spectrum of 3C 273 is so important. For the first time, we can measure absorbing systems down to a completeness limit of $\log N_{\text{HI}} \approx 12.3$, thereby probing these weak absorbers that are predicted to be physically equivalent to high-redshift forest absorbers.

Table 1: Observational & archival studies of the Lyman Forest toward 3C 273

Inst	Obs/ Arch	$\lambda\lambda$ (\AA)	Res (km/s)	S/N	Reference
FOS	Obs	1150-1600	~ 240	48	Bahcall et al. 1991
FOS	Arch				Bahcall et al. 1993
GHR	Obs	1175-1452	~ 200	30	Morris et al. 1991
GHR	Obs	1235-1425	>20	9	Brandt, Heap et al. 1993
GHR	Arch				Morris et al. 1993
GHR	Arch				Brandt, Heap et al. 1997
GHR	Obs	1215-1250	>20	9	Weymann, Rauch et al. 1995
GHR	Arch				Grogin & Geller 1998
GHR	Arch				Penton, Stocke et al. 2000
GHR	Arch				Penton, Shull et al. 2000
FUSE	Obs	900-1190	20	15-35	Sembach et al. 2001
STIS	Obs	1150-1700	7	30-44	Heap et al. 2001 (in prep)

2. Observations

To observe 3C 273 we used STIS in the E140M mode, which yields an echelle spectrogram covering the spectral range, 1150–1700 \AA . The nominal two-pixel resolution of this mode is 7 km/s, but in our case, the effective resolving power was slightly less because we used a “large” $0''.2$ aperture and therefore lost some spectral purity. We observed 3C273 during two visits spaced a few months apart, the first one lasting 2 orbits, the second, for 5 orbits. The total exposure time was 18,671 sec. The two visits have the spectrum on different regions of the detector format, which means that every point in the spectrum was viewed by two different regions of the detector. This redundancy made it easier to identify and account for detector blemishes and fixed-pattern noise.

We reduced the data using software developed at Goddard by the STIS Instrument Definition Team (Lindler 1998). Individual orders of the echellogram were extracted and calibrated, and corrections for scattered light were then applied. We combined the 7 orbits of data for each spectral order, with weighting based on a pixel’s signal-to-noise. We then coadded the spectral orders to form a single, continuous spectrum. The S/N per pixel rises from ~ 20 at 1230 \AA to ~ 29 at 1380 \AA , although there is significant variation in S/N within each order. Equivalently, the S/N per 7-km/s resolution element is 30 – 44.

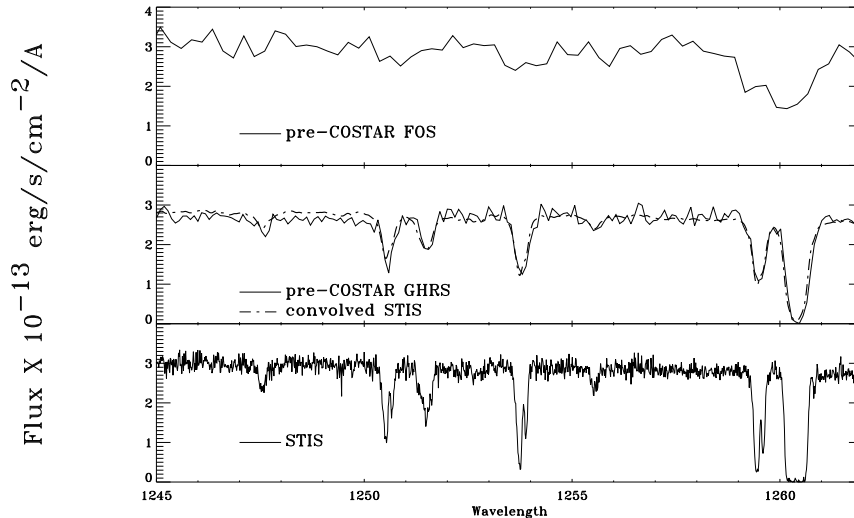


Figure 1. FOS (top), GHRs (middle), and STIS (bottom) spectra of 3C 273. The middle panel also shows our STIS spectrum convolved with the line-spread function of the pre-COSTAR GHRs (Heap et al. 1995). The features at 1250.5, 1253.8, 1259.5, and 1260.4 Å are interstellar.

Figure 1 compares a segment of the final STIS spectrum with those from the FOS and GHRs. It demonstrates the marked improvement in S/N and resolution over previous spectrographs. Actually, the comparison with GHRs (middle panel) is a little unfair, since the only GHRs spectra of 3C 273 were taken before the COSTAR corrective optics were deployed. Nevertheless, it shows that pre-COSTAR GHRs spectra couldn't resolve features into multiple components as STIS can. In fact, STIS can resolve virtually all Ly α absorbers.

3. Simulations

In parallel with STIS data analysis, we generated 20 artificial STIS spectra drawn from a simulation of a Λ CDM universe (see Davé et al. 1999 for simulation parameters). By comparing the statistical properties of the observed and artificial spectra, we can in principle (i) constrain the parameters of the Λ CDM model and (ii) infer physical conditions in the local intergalactic medium.

It is crucial that the simulations be faithful reproductions of STIS data if they are to be of any value. We therefore took great pains to account for all the characteristics and foibles of STIS data. Figure 2 illustrates some of the steps to compute the simulated STIS spectra. First, we took a normalized simulated spectrum (top panel) and put it on an absolute flux scale. We then constructed the corresponding STIS echellograms (one for each visit) complete with scattered light, noise as appropriate, and interstellar lines added in. We next reduced the echellograms in exactly the same way as for a STIS observation

and estimated the continuum level (middle panel). The bottom panel shows the final, normalized STIS spectrum ready for measurement with AutoVP (Davé et al. 1997).

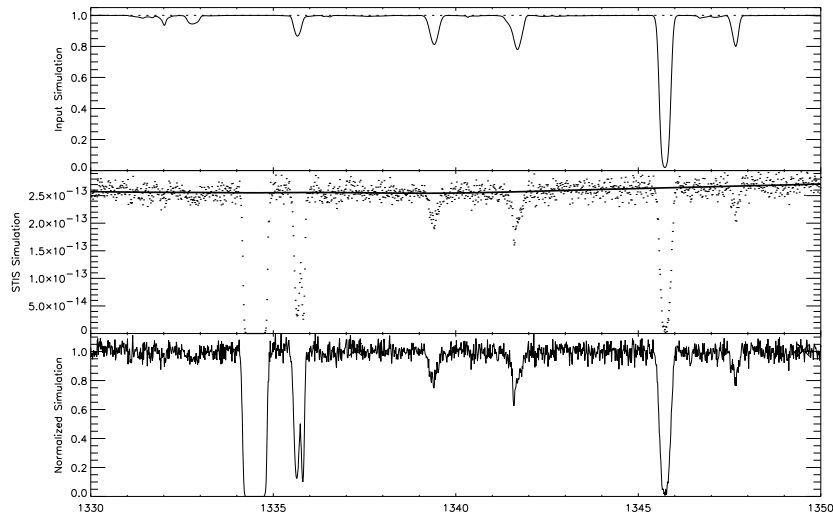


Figure 2. Portion of a simulated spectrum. The three panels show the original, normalized simulated spectrum (top), the STIS simulation with estimated continuum (middle), and the final, normalized STIS simulated spectrum. The strong features near 1335\AA are interstellar CII lines that has been added to the artificial spectrum.

4. Measurements

The preliminary results presented here are based on Davé’s method for defining the continuum using an automated median filter, then using AutoVP to detect absorption features and determine their column densities (N_{HI}) and Doppler parameters (b). Independently, GW and SRH also defined the continuum level (using manual procedures), identified absorption systems, and measured line parameters. We are now in the process of comparing our results in detail, but one early finding is that lines that are unsaturated and isolated (which constitute most of the intergalactic absorbers detected) have line parameters that are consistent within errors between these three independent estimates.

RD has recently modified AutoVP in an attempt to identify more broad, weak absorbers that may arise in shock-heated intergalactic gas (e.g. Tripp, Savage & Jenkins 2000). In particular, AutoVP now uses a variable-width Gaussian detection window rather than a narrow, fixed-width boxcar window, as in previous studies such as Davé & Tripp (2001). We are in the process of extensively testing the effects of this new algorithm, but preliminary results seem to indicate that significantly more broad, weak absorbers are now detected.

b - N_{HI} distributions are one way to gain information about the “effective equation of state” of the IGM at low-redshift. Since the narrowest absorbers are presumably purely thermally broadened, the lower envelope of the b - N_{HI} distribution gives a measure of the temperature of Ly α absorbing gas that has not been shock-heated (Hui & Gnedin 1997).

How much faith should we put in our b - N_{HI} measurements? The FUSE Ly β survey should give us pause. Shull et al. (2000; this conference) found that Doppler widths of *saturated* lines ($\log N_{\text{HI}} \gtrsim 13.7$) derived from Ly β /Ly α equivalent-width ratios were systematically lower than from Ly α profile analysis of GHR spectra; consequently, the FUSE column densities are higher. This appears to be the case with 3C 273 as well. Penton et al. (2000a,b) derived high Doppler widths ($b \sim 60 - 80$ km/s) for 13 Ly α lines detected in pre-COSTAR GHR spectra of 3C 273, whereas Sembach et al. (2001) got much lower Doppler widths from Ly β /Ly α ratios in the FUSE spectrum for the 8 strong absorbers in common.

Fortunately, the situation is not as serious as would appear at first glance – at least for 3C 273. Our b estimates from STIS spectra generally agree within the quoted 1σ errors with the COG estimates from FUSE. The only exception is the strong, saturated absorber at 1222Å (which is not included in our study). The spurious GHR results were caused by a failure to account for the blurring of pre-COSTAR spectra (Fig. 1). They are not relevant to our study since most (97%) of the Ly α lines in the STIS spectrum are unsaturated and should therefore have reliable line parameters.

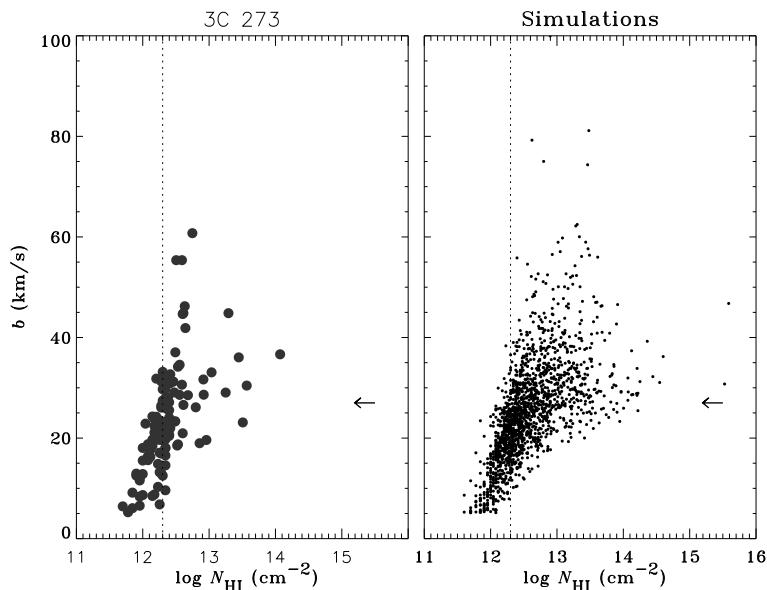


Figure 3. N_{HI} - b for the 3C 273 observations vs. simulations. The vertical dotted line indicates the estimated completeness limit ($\log N_{\text{HI}}=12.3$); the horizontal arrow, the measured median Doppler width of lines above the completeness limit (med. $b=27$ km/s for both observations and simulations).

5. Results

Figure 3 shows our measured b - N_{HI} distributions for 3C 273 and the simulations. Both distributions show a strong correlation between column density and linewidth. The median Doppler width in the simulations, where we have better statistics, increases quickly from about 20 km/s at $N_{\text{HI}}=12.3$ to 30 km/s at $N_{\text{HI}}=13.0$, then begins to level off for $N_{\text{HI}} \gtrsim 14.0$. The levelling off suggests that these high column density absorbers are probing gas associated with galaxies, and is not heated by the metagalactic ultraviolet flux.

The median Doppler width found for 3C273 is significantly higher than what Davé & Tripp (2001) measured from STIS spectra of PG0953 and H1821 (Table 2). This difference likely reflects the new line-detection algorithm in AutoVP described earlier. In fact, a reanalysis of the Davé & Tripp data set with the new AutoVP also finds a higher median $b \approx 26$ km/s. This example illustrates how specific algorithmic choices can have a significant impact on line parameters and resulting interpretations, a fact that is well-known in high-redshift forest studies (motivating, for instance, the use of flux-based statistics).

Table 2: Comparison with other studies

Reference	$\log N_{\text{HI}}$ range	z	β	med. b
Kim et al. (2001)	12.5-14.0	2.1	1.38 ± 0.08	25
Kim et al. (2001)	12.5-14.0	1.6	1.72 ± 0.16	28
Shull (this conf.)	12.3-14.0	< 0.1	1.82 ± 0.10	25*
Davé & Tripp (2001)	13.0-14.5	0.17	2.04 ± 0.23	21
This paper	12.3-14.0	< 0.1	2.02 ± 0.21	27

*value assumed for COG estimation of $\log N_{\text{HI}}$

The top panel of Figure 4 shows the number density distribution, $\mathcal{N}(N_{\text{HI}}) = AN_{\text{HI}}^{-\beta}$, for both 3C 273 and the simulations. The turnover in this distribution at low column densities allows a rough estimate of the completeness limit of lines, and is seen to be roughly $N_{\text{HI}} \approx 10^{12.3} \text{ cm}^{-2}$; we are working on a more thorough analysis of completeness in this sample. The observed slope for 3C 273, $\beta \approx 2.0$ is slightly steeper than that estimated by Penton et al. (2000; c.f. Shull, this conference) but is nearly exactly the same as that found by Davé and Tripp (Table 2).

Both our observations and simulations have slopes ($\beta_{\text{obs}} = 2.02 \pm 0.21$, $\beta_{\text{sim}} = 1.90 \pm 0.04$) that are significantly steeper than at $z > 2$ (see Table 2). At higher column densities, the $\mathcal{N}(N_{\text{HI}})$ distribution flattens somewhat ($\beta = 1.42 \pm 0.16$ according to Shull, this conference) and comes into basic agreement with the high-redshift slope (Kim et al. 2001). The steeper slope at low column densities indicates that higher column-density lines are evolving away faster than are lower column-density ones, in agreement with findings from the HST Quasar Absorption-Line Key Project (Weymann et al. 1998).

The agreement in amplitude indicates that the ionizing background assumed in the simulations is close to correct (within the framework of this cosmology and simulation; see discussion in Davé & Tripp); it seems to suggest the intensity predicted by Haardt & Madau (1996) is roughly correct (within a factor of a few), as suggested by the analysis of Davé & Tripp.

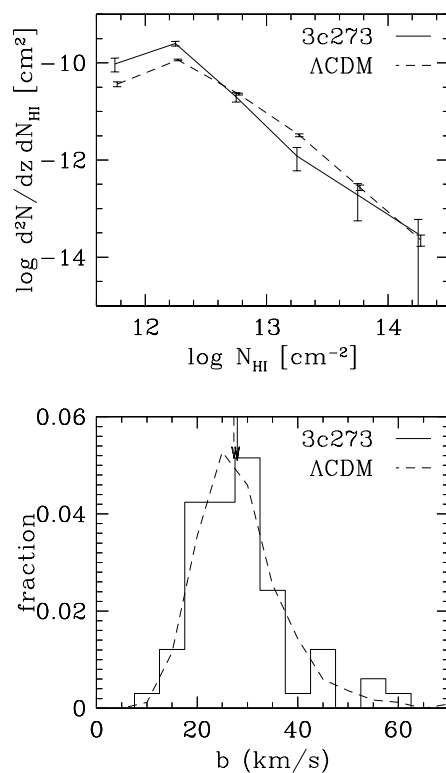


Figure 4. Column density distributions (top) and Doppler-width distributions (bottom). In both panels, the observations are indicated by the solid line, and the simulations, by the dashed line.

References

- Bahcall, J. et al. 1991, ApJ, 377, L5
 Bahcall, J. et al. 1993, ApJS, 87,1
 Bechtold, J., Weymann, R.J., Lin, Z., Malkan, M. 1987, ApJ, 315, 180
 Brandt, J., Heap, S. et al. 1993, AJ, 105, 831
 Brandt, J., Heap, S. et al. 1997, AJ, 114, 554
 Davé, R., Hernquist, L., Weinberg, D., & Katz, N. 1997, ApJ, 477, 21
 Davé, R., Hernquist, Katz, N., Weinberg, D. 1999, ApJ, 511, 521
 Davé, R., & Tripp, T. 2001, astro-ph 0101419
 Grogin, N. & Geller, M. 1998, ApJ, 505, 506
 Heap, S., Brandt, J., et al. 1998, PASP, 107, 871
 Hui, L. & Gnedin, N. 1997, MNRAS, 292, 27

- Kim, T.-S., Christiani, S., D'Odorico, S. 2001, *A&A*, 373, 757
- Lindler, D. J. 1998, <http://hires/stis/docs/calstis/calstis.html>
- Morris, S., Weymann R., et al. 1991, *ApJ*, 377, L21
- Morris, S., Weymann R., et al. 1993, *ApJ*, 419, 524
- Penton, S., Stocke, J., & Shull, J.M. 2000, *ApJS*, 130, 121
- Penton, S., Shull, J.M., & Stocke, J. 2000, *ApJ*, 544, 150
- Sembach, K. et al. 2001, *ApJ*, in press; astro-ph/0108047
- Shull, J.M., Giroux, M., Penton, S. et al. 2000, *ApJ*, 538, 13
- Shull, J.M. 2001, astro-ph/0107473
- Tripp, T. M., Savage, B. D., & Jenkins, E. B. 2000, *ApJ*, 534, L1
- Weymann, R., Rauch, M. et al. 1995, *ApJ*, 438, 650
- Weymann, R., Jannuzi, B., Lu, L. et al. 1998, *ApJ*, 506, 1